

Artificial Neural Network for predicting Flexural Strength of Concrete Containing Cr₂O₃ Nanoparticles

Farzad Soleymani¹ and Akbar Karimi Livary²

1) Department of Metallurgical Engineering, Payame Noor University, P.O. 19395-4697, Tehran, Iran.

2) Department of Materials Engineering, Saveh Branch, Islamic Azad University, Saveh, Iran.

E-mail: farzad.soleymani52@yahoo.com

Abstract: In the present paper, a model based on artificial neural networks (ANN) for predicting flexural strength of concretes containing Cr₂O₃ nanoparticles have been developed at different ages of curing. For purpose of building these models, training and testing using experimental results for 144 specimens produced with 16 different mixture proportions were conducted. The data used in the multilayer feed forward neural networks models and inputvariables of genetic programming models are arranged in a format of eight input parameters that cover the cement content (C), nanoparticle content (N), aggregate type (AG), water content (W), the amount of superplasticizer (S), the type of curing medium (CM), Age of curing (AC) and number of testing try (NT). According to the input parameters, in the model the flexural strength of concretes was predicted. Neural network have trained results good and the new data can be predicted by the trained network as well.

[Farzad Soleymani. **Artificial Neural Network for predicting Flexural Strength of Concrete Containing Cr₂O₃ Nanoparticles.** *J Am Sci* 2012;8(8):155-162]. (ISSN: 1545-1003). <http://www.jofamericanscience.org>. 24

Keywords: Concrete; Cr₂O₃ nanoparticles; artificial neural network; genetic programming; flexural strength

1. Introduction

Strength assessment of concrete is a main and probably the most important mechanical property, which is usually measured after a standard curing time. Concrete strength is influenced by lots of factors like concrete ingredients, age, ratio of water to cementitious materials, etc. The pore structure determines the transport properties of cement paste, such as permeability and ion migration. Permeability of cement paste is a fundamental property in view of the durability of concrete: it represents the ease with which water or other fluids can move through concrete, thereby transporting aggressive agents. It is therefore of utmost importance to investigate the quantitative relationships between the pore structure and the permeability. Through experimental studies and then numerical simulations of the pore structure and the permeability of cement-based materials, a better understanding of transport phenomena and associated degradation mechanisms will hopefully be reached [1].

Conventional methods of predicting various properties of concrete are generally based on either water to cement ratio rule or maturity concept of concrete [2]. Over the last two decades, a different modeling method based on neural networks (NNs) has become popular and used by many researchers for a wide range of engineering applications. NNs are a family of massively parallel architectures that solve difficult problems via the cooperation of highly interconnected but simple computing elements (or artificial neurons). Basically, the processing elements of a neural network are analogous to the neurons in the brain, which consist of many simple computational elements arranged in several layers [3]. The concrete

properties could be calculated using the models built with NNs. It is convenient to use these models for numerical experiments to review the effects of each variable on the mix proportions [4-6]. The aim of this study is to predict flexural strength of several types of concrete with and without Cr₂O₃ nanoparticles by ANNs. Totally 144 flexural strength data from 16 different concrete mixtures were collected, trained and tested by means of different models. The obtained results have been compared by experimental ones to evaluate the software power for predicting the properties of concrete.

2. Experimental procedure

2.1. Materials

Two series of concrete were made in the laboratory. The first was normally vibrated concrete (NVC) series with ordinary river sand as aggregates and the second self compacting concrete (SCC) series with limestone aggregates. The utilized materials are as below:

Ordinary Portland Cement (OPC) conforming to ASTM C150 [7] standard was used as received. The chemical and physical properties of the cement are shown in Table 1. The particle size distribution pattern of the used OPC has been illustrated in Fig. 1.

Cr₂O₃ nanoparticles with average particle size of 15 nm and 45 m²/g Blaine fineness producing from Suzhou Fuer Import & Export Trade Co., Ltd was used as received. The properties of Cr₂O₃ nanoparticles are shown in Table 2. Scanning electron micrographs (SEM) and powder X-ray diffraction (XRD) diagrams of Cr₂O₃ nanoparticles are shown in Figs. 2 and 3.

Table 1. Chemical and physical properties of Portland cement (Wt. %)

| Material | SiO ₂ | Al ₂ O ₃ | Cr ₂ O ₃ | CaO | MgO | SO ₃ | Na ₂ O | K ₂ O | Loss on ignition |
|----------|------------------|--------------------------------|--------------------------------|-------|------|-----------------|-------------------|------------------|------------------|
| Cement | 21.89 | 5.3 | 3.34 | 53.27 | 6.45 | 3.67 | 0.18 | 0.98 | 3.21 |

Specific gravity: 1.7 g/cm³Table 2. The properties of nano- Cr₂O₃

| Diameter (nm) | Surface Volume ratio (m ² /g) | Density (g/cm ³) | Purity (%) |
|---------------|--|------------------------------|------------|
| 15 ± 3 | 155 ± 12 | < 0.13 | >99.9 |

Table 3. Physical and chemical characteristics of the polycarboxylate admixture.

| | |
|----------------------------|---------------------|
| Appearance | Yellow-brown liquid |
| % solid residue | Approximately 36% |
| pH | 5.2-5.3 |
| Specific gravity (kg/l) | Approximately 1.06 |
| Rotational Viscosity (MPa) | 79.30 |
| % C | 52.25 |
| ppm Na ⁺ | 9150 |
| ppm K ⁺ | 158 |

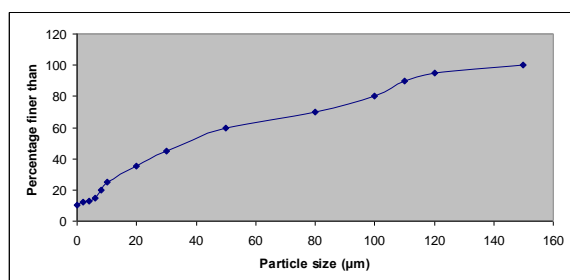
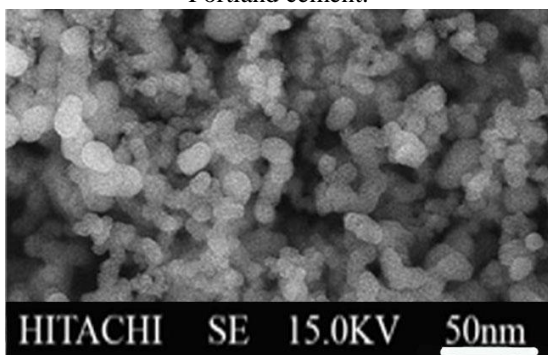
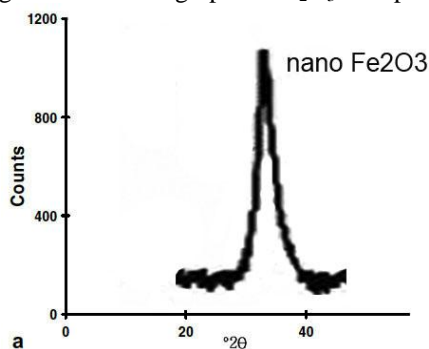


Fig.1. Particles distribution pattern of ordinary Portland cement.

Fig. 2. SEM micrograph of Cr₂O₃ nanoparticles.Fig. 3. XRD analysis of Cr₂O₃ nanoparticles.

Locally available natural sand with particles smaller than 0.5 mm and fineness modulus of 2.25 and specific gravity of 2.58 g/cm³ was used as fine aggregate for NVC series concrete. Crushed basalt stored in the laboratory with maximum size of 15 mm and specific gravity of 2.96 g/cm³ was used as coarse aggregate in NVC series concrete.

Crushed limestone aggregates were used to produce self-compacting concretes, with gravel 4/12 and two types of sand: one coarse 0/4, for fine aggregates and the other fine 0/2, with a very high fines content (particle size < 0.063 mm) of 19.2%, the main function of which was to provide a greater volume of fine materials to improve the stability of the fresh concrete. A polycarboxylate with a polyethylene condensate defoamed based admixture (Glenium C303 SCC) was used. Table 3 shows some of the physical and chemical properties of polycarboxylate admixture used in this study.

2.2. Mixture proportions

Totally 6 series of mixtures were prepared and tested experimentally. C0 series mixtures were prepared as control specimens. The control mixtures were made of natural aggregates, cement and water. C0 series mixtures were cured in water (W) and saturated limewater (LW) and designated as C0-W and C0-LW series, respectively. N series were prepared with different contents of Cr₂O₃ nanoparticles. The mixtures were prepared by the cement replacement of 0.5, 1.0, 1.5 and 2.0 weight percent. N series mixtures were also cured in water (W) and saturated limewater (LW) and designated as N-W and N-LW series, respectively.

C0-SCC series mixtures were prepared by cement, fine and ultra-fine crushed limestone aggregates with 19.2% by weight of ultra-fine ones and 1.0 weight percent of polycarboxylate admixture replaced by

water. N-SCC series were prepared with different contents of Cr_2O_3 nanoparticles. The mixtures were prepared with the cement replacement by Cr_2O_3 nanoparticles from 1 to 5 weight percent and 1 weight percent polycarboxylate admixture.

The water to binder ratio for all mixtures was set at 0.40. The binder content of all mixtures was 450 kg/m^3 . The proportions of the mixtures are presented in Table 4.

2.3. Test procedure

For NVC series concrete, cubes with $200 \text{ mm} \times 50 \text{ mm} \times 50 \text{ mm}$ edges were cast and compacted in two layers on a vibrating table, where each layer was vibrated for 10 s. SCC series mixtures were prepared without subsequent vibration. The moulds were covered with polyethylene sheets and moistened for 24 h. Then the specimens were demolded and cured in water and saturated limewater at a temperature of 20°C prior to test days.

Flexural tests were carried out according to the ASTM C 293 [8] standard. After the specified curing period was over (7, 28 and 90 days for NVC series and 2, 28 and 90 days for SCC series), the concrete cubes were subjected to flexural test by using universal testing machine. The tests were carried out triplicately.

3. Experimental results

The flexural strength results of the specimens are shown in Table 4. Table 4 shows that the flexural strength increases with adding nano- Cr_2O_3 particles up to 1.0% in N-W series. It is shown that using 2.0% Cr_2O_3 nanoparticles decreases the flexural strength to a value which is near to the control concrete. This may be due to the fact that the quantity of nano- Cr_2O_3 particles is higher than the amount required to combine with the liberated lime during the process of hydration thus leading to excess silica leaching out and causing a deficiency in strength as it replaces part of the cementitious material but does not contribute to strength [10]. Also, it may be due to the defects generated in dispersion of nanoparticles that causes weak zones. The high enhancement of flexural strength in the N series blended concrete are due to the rapid consuming of $\text{Ca}(\text{OH})_2$ which was formed during hydration of Portland cement specially at early ages related to the high reactivity of nano- Cr_2O_3 particles. As a consequence, the hydration of cement is accelerated and larger volumes of reaction products are formed. Also nano- Cr_2O_3 particles recover the particle packing density of the blended cement, directing to a reduced volume of larger pores in the cement paste.

On the other hand, for the specimens saturated in limewater, the flexural strength increases by adding up to 2.0 weight percent Cr_2O_3 nanoparticles. Lime reacts with water and produces $\text{Ca}(\text{OH})_2$ which needs to form

strengthening gel. When Cr_2O_3 nanoparticles react with $\text{Ca}(\text{OH})_2$ produced from saturated limewater, the content of strengthening gel is increased because of high free energy of nanoparticles which reduces significantly when reacts by $\text{Ca}(\text{OH})_2$.

Table 4 also shows the flexural strength of C0-SCC and N-SCC specimens at 2, 7 and 28 days of curing. The results show that the flexural strength increases by adding Cr_2O_3 nanoparticles up to 4.0 weight percent replacements (N4-SCC series) and then it decreases, although adding 5.0 percent Cr_2O_3 nanoparticles produces specimens with much higher flexural strength with respect to C0-SCC and N-SCC specimens with 1.0, 2.0 and 3.0 weight percent Cr_2O_3 nanoparticles.

The mechanism that the nanoparticles improve the strength of concrete specimens can be interpreted as follows [13]: Suppose that nanoparticles are uniformly dispersed in concrete and each particle is contained in a cube pattern, therefore the distance between nanoparticles can be determined. After the hydration begins, hydrate products diffuse and envelop nanoparticles as kernel [13]. If the content of nanoparticles and the distance between them are appropriate, the crystallization will be controlled to be a suitable state through restricting the growth of $\text{Ca}(\text{OH})_2$ crystal by nanoparticles. Moreover, the nanoparticles located in cement paste as kernel can further promote cement hydration due to their high activity. This makes the cement matrix more homogeneous and compact. Consequently, the strength of concrete is improved evidently such as the concrete containing nano- Cr_2O_3 in the amount of 1% by weight of binder [13].

With increasing the content of Cr_2O_3 nanoparticles more than a specific weight percent (based on the concrete type), the improvement on the strength is weakened. This can be attributed to that the distance between nanoparticles decreases with increasing content of nanoparticles, and $\text{Ca}(\text{OH})_2$ crystal cannot grow up enough due to limited space and the crystal quantity is decreased, which leads to the ratio of crystal to strengthening gel small and the shrinkage and creep of cement matrix increased [14], thus the strength of cement matrix is looser relatively.

On the whole, the addition of nanoparticles improves the strength of concrete. On the one hand, nanoparticles can act as a filler to enhance the density of concrete, which leads to the porosity of concrete reduced significantly. On the other hand, nanoparticles can not only act as an activator to accelerate cement hydration due to their high activity, but also act as a kernel in cement paste which makes the size of $\text{Ca}(\text{OH})_2$ crystal smaller and the tropism more stochastic.

Table 4. Average flexural strength of different mixture proportion of concrete specimens

| Sample designation | Cr ₂ O ₃ nanoparticles (%) | PC content (%) | Quantities (kg/m ³) | | Average Flexural Strength (MPa) | | | |
|--------------------|--|----------------|---------------------------------|--|---------------------------------|--------|---------|---------|
| | | | Cement | Cr ₂ O ₃ nanoparticles | 2 days | 7 days | 28 days | 90 days |
| C0-W | 0 | 0 | 450.00 | 0.00 | - | 4.2 | 4.4 | 4.7 |
| N1-W | 0.5 | 0 | 447.75 | 2.25 | - | 4.9 | 5.0 | 5.7 |
| N2-W | 1.0 | 0 | 445.50 | 4.50 | - | 5.4 | 5.2 | 6.0 |
| N3-W | 1.5 | 0 | 443.25 | 6.75 | - | 5.0 | 5.0 | 5.3 |
| N4-W | 2.0 | 0 | 441.00 | 9.00 | - | 4.3 | 4.8 | 5.0 |
| C0-LW | 0 | 0 | 450.00 | 0.00 | - | 4.0 | 4.1 | 4.2 |
| N1-LW | 0.5 | 0 | 447.75 | 2.25 | - | 5.2 | 5.5 | 5.7 |
| N2-LW | 1.0 | 0 | 445.50 | 4.50 | - | 5.8 | 5.9 | 6.0 |
| N3-LW | 1.5 | 0 | 443.25 | 6.75 | - | 6.3 | 6.4 | 6.3 |
| N4-LW | 2.0 | 0 | 441.00 | 9.00 | - | 6.8 | 7.0 | 7.2 |
| C0-SCC1 | 0 | 1.0 | 450.00 | 0.00 | 2.8 | 3.7 | 4.2 | - |
| N1-SCC1 | 1 | 1.0 | 445.50 | 4.50 | 3.2 | 4.3 | 4.7 | - |
| N2-SCC1 | 2 | 1.0 | 441.0 | 9.00 | 3.5 | 4.6 | 5.8 | - |
| N3-SCC1 | 3 | 1.0 | 437.5 | 13.50 | 3.6 | 5.0 | 6.7 | - |
| N4-SCC1 | 4 | 1.0 | 432.0 | 18.00 | 3.9 | 5.7 | 7.4 | - |
| N5-SCC1 | 5 | 1.0 | 427.5 | 22.50 | 3.7 | 5.4 | 7.1 | - |

Water to binder [cement + nano- Cr₂O₃] ratio of 0.40

W denotes the specimens cured in water and LW denotes to those cured in saturated limewater

4. Artificial Neural Networks

ANNs were developed to model the human brain [15]. Even an ANN fairly simple and small in size when compared to the human brain, has some powerful characteristics in knowledge and information processing because of its similarity to the human brain. Therefore, an ANN can be a powerful tool for engineering applications [16]. McCulloch and Pitts [17] defined artificial neurons for the first time and developed a neuron model as in Fig. 4. McCulloch and Pitts' network [17] formed the basis for almost all later neural network models. Afterwards, Rosenblatt [18] devised a machine called the perceptron that operated much in the same way as the human mind. Rosenblatt's perceptrons [11] consist of "sensory" units connected to a single layer of McCulloch and Pitts [12] neurons. Rumelhardt et al. [13] derived a learning algorithm for perceptron networks with constituted hidden units. Their learning algorithm is called back-propagation and is now the most widely used learning algorithm. Fig. 5 is shown a typical architecture of a multilayer perceptron neural network with an input layer, two hidden layer and one output layer. As a result of these studies, together with the developments in computer technology, using ANN has become more efficient after 1980 [14].

As it can be seen from Fig. 4, an artificial neuron is composed of five main parts: inputs, weights, sum function, activation function and outputs. Inputs are information that enters the neuron from other neurons or from external world. Weights are values that express the outcome of an input set or another process

element in the preceding layer on this process element. Sum function is a function that calculates the effect of inputs and weights completely on this process element. This function computes the net input that approaches to a neuron [15]. The weighted sums of the input components (net_j) are calculated using Eq. (1) as follows:

$$(net)_j = \sum_{i=1}^n W_{ij} x_i + b \quad (1)$$

where (net_j) is the weighted sum of the j th neuron for the input received from the preceding layer with n neurons, W_{ij} is the weight between the j th neuron in the previous layer, x_i is the output of the i th neuron in the previous layer [14]. b is a fix value as internal addition and Σ represents sum function. Activation function is a function that processes the net input obtained from sum function and determines the neuron output. In general for multilayer feed-forward models as the activation function sigmoid activation function is used. The output of the j th neuron (out_j) is computed using Eq. (2) with a sigmoid activation function as follows [16]:

$$O_j = f(net)_j = \frac{1}{1 + e^{-\alpha(net)_j}} \quad (2)$$

where α is constant used to control the slope of the semi-linear region. The sigmoid nonlinearity activates in every layer except in the input layer [14]. The sigmoid activation function represented by Eq. (2) gives outputs in (0, 1). If it desired, the outputs of this function can be adjusted to (-1,1) interval. As the sigmoid processor represents a continuous function it is particularly used in non-linear descriptions. Because

its derivatives can be determined easily with regard to the parameters within (net)_j variable [14].

LMBP is often the fastest available back-propagation algorithm, and is highly recommended as a first-choice supervised algorithm, although it requires more memory than other algorithms. The standard LMBP training process can be described in the pseudocode of Fig. 6 [17].

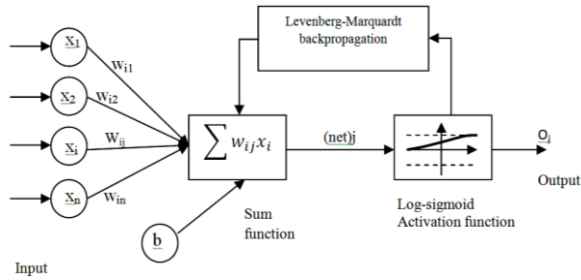


Fig. 4. Architecture of applied neural network.

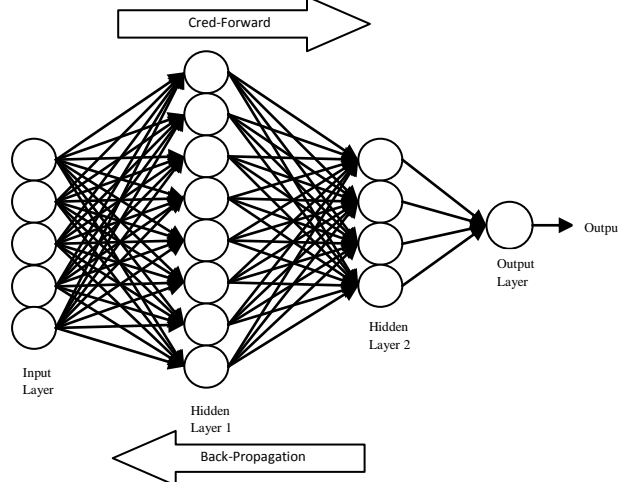


Fig. 5. A typical architecture of multilayer perceptron neural network.

4.1. Neural network model structure and parameters

ANN model is carried out in this research has eight neurons in the input layer and one neurons in the output layer as demonstrated in Fig. 7. The values for input layers were cement content (C), nanoparticle content (N), aggregate type (AG), water content (W), the amount of superplasticizer (S), the type of curing medium (CM), Age of curing (AC) and number of testing try (NT). The values for output layer were flexural strength (f_F) in the other set. Two hidden layer with ten and eight neurons were used in the architecture of multilayer neural network because of its minimum absolute percentage error values for training and testing sets. The neurons of neighboring layers are completely interconnected by weights. Finally, the output layer neurons produce the network prediction as a result.

In this study, the back-propagation training algorithm has been utilized in feed-forward two hidden layers. Back-propagation algorithm, as one of the most well-known training algorithms for the multilayer perceptron, is a gradient descent technique to minimize the error for a particular training pattern in which it adjust the weights by a small amount at a time [17]. The non-linear sigmoid activation function was used in the hidden layer and the neuron outputs at the output layer. Momentum rate and learning rate values were determined and the model was trained through iterations. The trained model was only tested with the input values and the predicted results were close to experiment results. The values of parameters used in neural network model are given in Table 5.

To make a decision on the completion of the training processes, two termination states are declared: state 1 (ANN-I model) means that the training of neural network was ended when the maximum epoch of process reached (1000) while state 2 (ANN-II model) means the training ended when minimum error norm of network gained.

5. Results

In this study, the error arose during the training and testing in ANN-I and ANN-II models can be expressed as absolute fraction of variance (R²) which are calculated by Eq. 3 [18]:

$$R^2 = 1 - \left(\frac{\sum_i (t_i - o_i)^2}{\sum_i (o_i)^2} \right) \tag{3}$$

where t is the target value, o is the output value and p is the pattern.

All of the results obtained from experimental studies and predicted by using the training and testing results of ANN I and ANN II models, are given in Figs. 8a and 8b. The linear least square fit line, its equation and the R² values were shown in these figures for the training and testing data. Also, inputs values and experimental results with testing results obtained from ANN-I and ANN-II models were given in Table 6. As it is visible in Fig. 8 the values obtained from the training and testing in ANN-I and ANN-II models are very close to the experimental results. The result of testing phase in Fig. 7 shows that the ANN-I and ANN-II models are capable of generalizing between input and output variables with reasonably good predictions.

The performance of the ANN-I and ANN-II models for f_F is shown in Fig. 8. The best value of R² is 96.41% for training set in the ANN-II model, The minimum value of R² is 85.47% for testing set in the ANN-I model. All of R² values show that the proposed ANN-I and ANN-II models are suitable and can predict f_F values for every age very close to the experimental values.

1. Initialize the weights and parameter μ ($\mu = 0.01$ is appropriate).
2. Compute the sum of the squared errors over all inputs $F(w)$

$$F(w) = e^T e \tag{3}$$
 Where $w = [w_1, w_2, \dots, w_n]$ consists of all weights of the network, e is the error vector comprising the error for all the training examples.
3. Solve (5) to obtain the increment of weights Δw

$$\Delta w = [J^T J + \mu I]^{-1} J^T e \tag{4}$$
 Where J is the Jacobian matrix, μ is the learning rate which is to be updated using the β depending on the outcome. In particular, μ is multiplied by decay rate β ($0 < \beta < 1$).
4. Using $w + \Delta w$ as the trial w , and judge
 IF trial $F(w) < F(w)$ in step 2 THEN

$$W = w + \Delta w$$

$$\mu = \mu \cdot \beta \quad (\beta = 0.1)$$

 go back to step 2
 ELSE

$$\mu = \mu / \beta$$

 go back to step 4
 END IF

Fig. 6. Pseudo-code for LMBP algorithm [19]

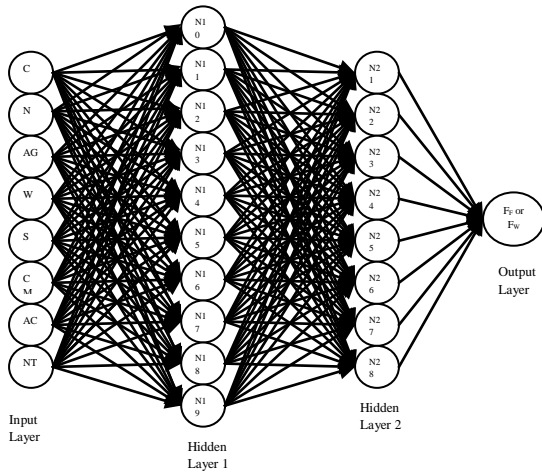
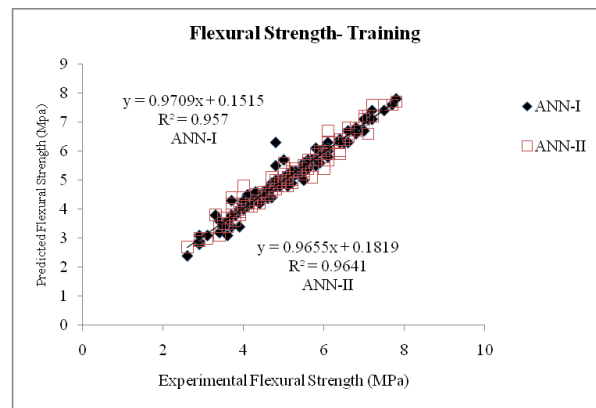


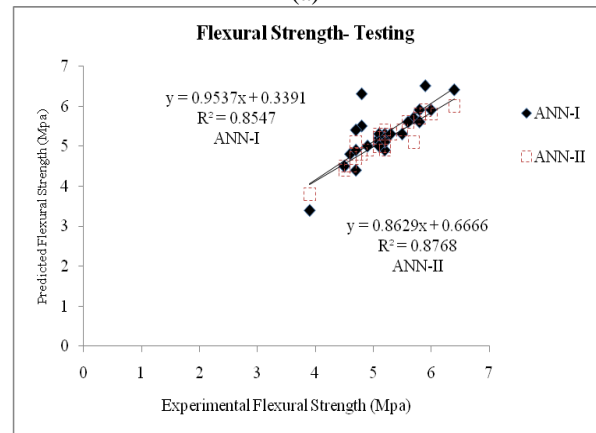
Fig. 7. The system used in the ANN model.

6. Discussion

Artificial neural networks are capable of learning and generalizing from examples and experiences. This makes artificial neural networks a powerful tool for solving some of the complicated civil engineering problems. In this study, using these beneficial properties of artificial neural networks in order to predict the flexural strength values of concretes containing Cr₂O₃ nanoparticles without attempting any experiments were developed two different multilayer artificial neural network architectures namely ANN-I and ANN-II. In two models developed in ANN method, a multilayered feed forward neural network with a back propagation algorithm was used. The models were trained with input and output data. Using only the input data in trained models the flexural strength of concrete specimens containing Cr₂O₃ nanoparticles were found.



(a)



(b)

Fig. 8. The correlation of the measured and predicted flexural strengths in a) training and b) testing phase for ANN models

Table 5. The values of parameters used in neural network model

| Parameters | ANN |
|-------------------------------------|----------|
| Number of input layer units | 8 |
| Number of hidden layer | 2 |
| Number of first hidden layer units | 10 |
| Number of second hidden layer units | 8 |
| Number of output layer units | 1 |
| Momentum rate | 0.88 |
| Learning rate | 0.70 |
| Error after learning | 0.000050 |
| Learning cycle | 30.000 |

Table 6. Testing data sets for comparison of experimental results with testing results predicted from models

| Cement (Kg/m ³) | Nano- Cr ₂ O ₃ (Kg/m ³) | Aggregate type | Water (Kg/m ³) | Superplasticizer (Kg/m ³) | Curing Medium | Age of Curing | No. Test try | Flexural Strength (MPa) | | |
|--------------------------------|---|-------------------|-------------------------------|--|------------------|------------------|--------------------|----------------------------|-----------|------------|
| | | | | | | | | Exp. | ANN- I | ANN- II |
| 450 | 0 | 3 | 0 | 18 | 1 | 7 | 3 | 4.6 | 4.6 | 4.7 |
| 450 | 0 | 3 | 0 | 18 | 1 | 28 | 3 | 4.6 | 4.8 | 4.5 |
| 447.75 | 2.25 | 3 | 0 | 18 | 1 | 7 | 2 | 4.7 | 5.4 | 4.8 |
| 447.75 | 2.25 | 3 | 0 | 18 | 1 | 28 | 3 | 5.1 | 5.2 | 5.2 |
| 447.75 | 2.25 | 3 | 0 | 18 | 1 | 90 | 3 | 5.9 | 6.5 | 5.9 |
| 445.5 | 4.5 | 3 | 0 | 18 | 1 | 7 | 3 | 5.6 | 5.6 | 5.6 |
| 445.5 | 4.5 | 3 | 0 | 18 | 1 | 28 | 1 | 5.1 | 5.3 | 5.3 |
| 445.5 | 4.5 | 3 | 0 | 18 | 1 | 90 | 2 | 5.8 | 5.9 | 5.8 |
| 443.25 | 6.75 | 3 | 0 | 18 | 1 | 7 | 2 | 5.1 | 5.1 | 5.0 |
| 443.25 | 6.75 | 3 | 0 | 18 | 1 | 28 | 1 | 5.1 | 5.0 | 5.2 |
| 441 | 9 | 3 | 0 | 18 | 1 | 7 | 1 | 3.9 | 3.8 | 4.0 |
| 441 | 9 | 3 | 0 | 18 | 1 | 90 | 1 | 4.8 | 4.8 | 4.8 |
| 450 | 0 | 3 | 0 | 18 | 2 | 90 | 2 | 4.4 | 4.2 | 4.4 |
| 447.75 | 2.25 | 3 | 0 | 18 | 2 | 7 | 2 | 5.4 | 5.3 | 5.0 |
| 447.75 | 2.25 | 3 | 0 | 18 | 2 | 28 | 1 | 5.7 | 5.6 | 5.3 |
| 445.5 | 4.5 | 3 | 0 | 18 | 2 | 7 | 3 | 5.9 | 5.8 | 5.8 |
| 443.25 | 6.75 | 3 | 0 | 18 | 2 | 90 | 1 | 5.9 | 5.9 | 6.0 |
| 441 | 9 | 3 | 0 | 18 | 2 | 28 | 2 | 6.9 | 6.9 | 6.9 |
| 450 | 0 | 4 | 0.18 | 17.82 | 1 | 7 | 2 | 4.1 | 3.9 | 4.0 |
| 445.5 | 4.5 | 4 | 0.18 | 17.82 | 1 | 7 | 2 | 4.0 | 4.2 | 4.1 |
| 445.5 | 4.5 | 4 | 0.18 | 17.82 | 1 | 28 | 1 | 4.3 | 4.4 | 4.4 |
| 441 | 9 | 4 | 0.18 | 17.82 | 1 | 7 | 2 | 4.6 | 4.4 | 4.7 |
| 441 | 9 | 4 | 0.18 | 17.82 | 1 | 28 | 3 | 6.2 | 5.9 | 6.1 |
| 437.5 | 13.5 | 4 | 0.18 | 17.82 | 1 | 28 | 1 | 6.3 | 6.4 | 6.4 |
| 432 | 18 | 4 | 0.18 | 17.82 | 1 | 7 | 2 | 5.7 | 5.6 | 5.6 |
| 427.5 | 22.5 | 4 | 0.18 | 17.82 | 1 | 2 | 2 | 3.7 | 3.8 | 3.7 |
| 427.5 | 22.5 | 4 | 0.18 | 17.82 | 1 | 28 | 1 | 6.6 | 6.7 | 7.3 |

The flexural strength and percentage of water absorption values predicted from training and testing, for ANN-I and ANN-II models, are very close to the experimental results. Furthermore, according to the flexural strength and percentage of water absorption results predicted by using ANN-I and ANN-II models, the results of ANN-II model are closer to the experimental results. R² values that are calculated for comparing experimental results with ANN-I and ANN-II model results have shown this situation.

7. Conclusions

1. Cr₂O₃ nanoparticles showed its influence on flexural strength and percentage water absorption up to 1.0 weight percent in N-W series concrete, up to 2.0 weight percent in N-LW series concrete and finally up to 4.0 weight percent in N-SCC series concrete. The deficiency in dispersion of nanoparticles more than the mentioned values causes the reduction of nanoparticles effects on improving flexural strength results.
2. ANN can be an alternative approach for the evaluation of the effect of cementitious material on the

flexural strength. There is an optimum replacement ratio of Cr_2O_3 nanoparticles existed; this value can be predicted using ANN models.

3. ANN efficient for predicting the flexural strength of Cr_2O_3 nanoparticles concrete.

References

- [1] Ye G, Lura P, van Breugel K. Modelling of water permeability in cementitious materials. *Materials and Structures* 2006; 39: 877–885.
- [2] Hong-Guang N, Ji-Zong W. Prediction of compressive strength of concrete by neural networks. *Cement Concr Res* 2000;30(8):1245–50.
- [3] Pala M, Ozbay O, Oztas A, Yuce MI. Appraisal of long-term effects of fly ash and silica fume on compressive strength of concrete by neural networks. *Construct Build Mater* 2005;21(2):384–94.
- [4] Akkurt S, Tayfur G, Can S. Fuzzy logic model for prediction of cement compressive strength. *Cement Concr Res* 2004;34(8):1429–33.
- [5] Baykasog˘lu A, Dereli T, Tamis_ S. Prediction of cement strength using soft computing techniques. *Cement Concr Res* 2004;34(11):2083–90.
- [6] Akkurt S, Ozdemir S, Tayfur G, Akyol B. The use of GA-ANNs in the modelling of compressive strength of cement mortar. *Cement Concr Res* 2003;33(7):973–9.
- [7] ASTM C150, Standard Specification for Portland Cement, annual book of ASTM standards, ASTM, Philadelphia, PA; 2001.
- [8] ASTM C39, Standard Test Method for Compressive Strength of Cylindrical Concrete Specimens, ASTM, Philadelphia, PA; 2001.
- [9] ASTM C642, Standard Test Method for Density, Absorption, and Voids in Hardened Concrete, ASTM, Philadelphia, PA; 2001.
- [10] Shih J.Y., Chang T.P. and Hsiao. T.C. "Effect of nanosilica on characterization of Portland cement composite", *Cement and Concrete Research*, Vol. 36. pp. 697 – 706, 2006.
- [11] Rosenblatt F. Principles of neuro dynamics: perceptrons and the theory of brain mechanisms. Washington, DC: Spartan Books; 1962.
- [12] McCulloch WS, Pitts W. A logical calculus of the ideas immanent in neural nets. *Bull Math Biophys* 1943;5:115–37.
- [13] Rumelhart DE, Hinton GE, William RJ. Learning internal representation by error propagation. In: Rumelhart DE, McClelland JL, editors. *Proceeding parallel distributed processing foundation*, vol. 1. Cambridge: MIT Press; 1986.
- [14] Liu SW, Huang JH, Sung JC, Lee CC. Detection of cracks using neural networks and computational mechanics. *Comput Meth Appl Mech Eng* 2002;191(25–26):2831–45.
- [15] Anderson JA. Cognitive and psychological computation with neural models. *IEEE Trans Syst Man Cybernetics*, V.SMC-13 1983;5:799–814.
- [16] Hopfield JJ. Neural networks and physical systems with emergent collective computational abilities. *Proc Nat Acad Sci* 1982;79:2554–8.
- [17] Suratgar AA, Tavakoli MB, Hoseinabadi A. Modified Levenberg–Marquardt method for neural networks training. *World Acad Sci Eng Technol* 2005;6:46–8.
- [18] Topcu IB, Sarıdemir M. Prediction of compressive strength of concrete containing fly ash using artificial neural network and fuzzy logic. *Comp Mater Sci* 2008;41(3):305–11.
- [19] Crrreira C. Gene expression programming: mathematical modeling by an artificial intelligence; 2002.

6/6/2012